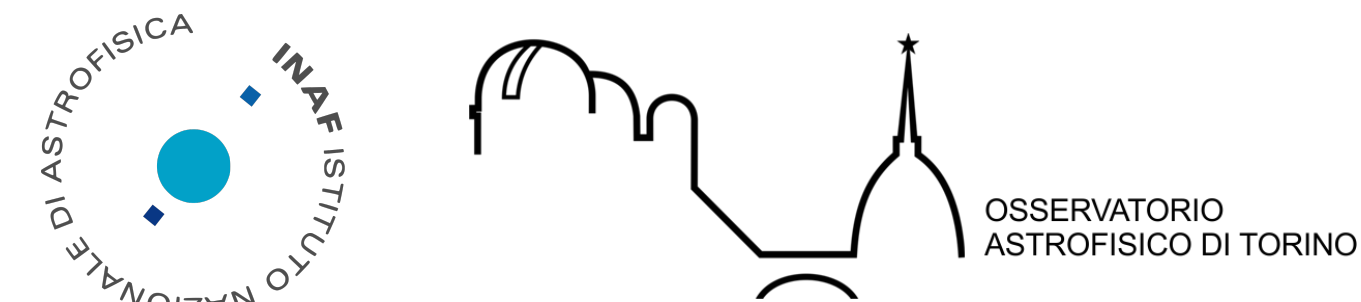


# DIAGNOSTICS OF CORONAL MASS EJECTIONS WITH SOLAR ORBITER/METIS



R. Susino and A. Bemporad  
INAF - Osservatorio Astrofisico di Torino



## Introduction

The analysis of the coronal emission observed at different wavelengths during the propagation of coronal mass ejections (CMEs) and associated phenomena, such as erupting prominences and shocks, can provide unique information on the main geometrical, kinetic, and thermodynamical properties of these major manifestations of the solar activity. We present recent results obtained from different diagnostic techniques applied to visible-light and UV coronagraphic data, providing physical properties of the plasma such as the density, temperature, and magnetic field distribution, in the perspective of the possible applications to future Solar Orbiter/Metis data.

## 3D structure of CMEs

Knowledge of the 3D structure of CMEs is fundamental to fix projection effects of 2D coronagraphic images and to derive directionality and real velocity of CMEs. Several techniques have been generally adopted: geometrical modelling, stereoscopy (with images from different viewpoints), polarisation ratio.

In particular, the polarisation-ratio method exploits the dependence of Thomson scattering on the scattering angle, hence on the location  $z$  of the electrons along the line of sight (LOS), since  $pB/B = f(z^2)$  (see Fig. 1).

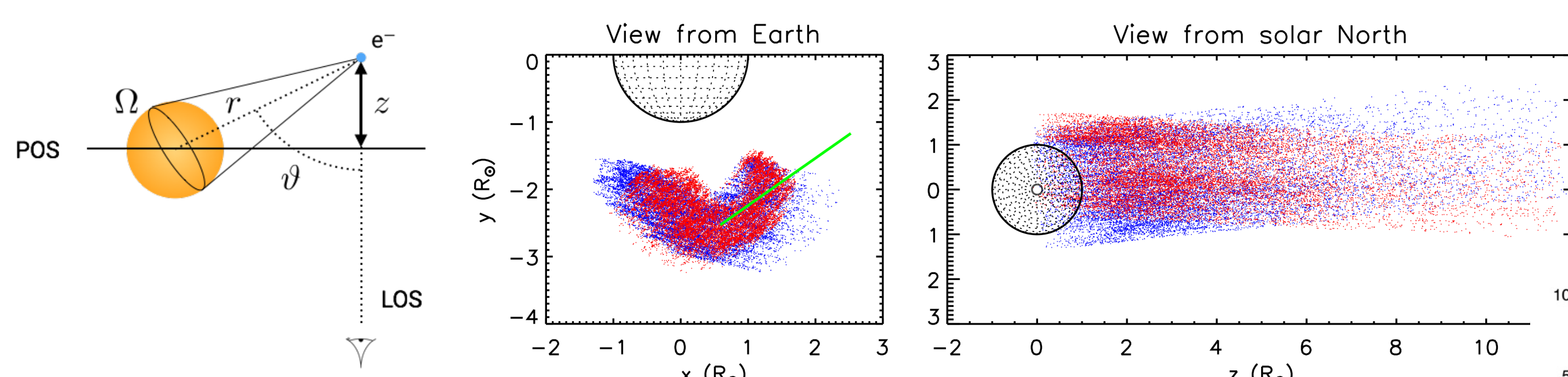


Figure 1. Left: geometry of the Thomson scattering. Right: example of 3D reconstruction using the polarisation-ratio method applied to polarised visible-light images of a CME acquired by STEREO-COR1. Left panel: view of the CME front from the Earth. Right panel: view of the CME front from above the ecliptic.

This method can be applied to single-viewpoint visible-light images of CMEs [1, 2]. Since CMEs are usually enclosed in a spatially limited region along the LOS, the measurement of the brightness ratio determines the weighted averaged distance from the plane of the sky (POS) of the emitting plasma [3]. In addition, statistical analysis to the whole distribution of identified scattering locations can be used to infer the depth along the LOS of the CME [1].

## Diagnostics of electron density

Computation of the electron density for transient events such as CMEs is usually performed from base-difference images that are related to the density in excess with respect to the ambient corona [4].

Base differences can only provide an estimate of the electron column density (units of  $\text{cm}^{-2}$ ), while the average density ( $\text{cm}^{-3}$ ) can be inferred only if the thickness of the CME plasma volume along the LOS is known. This estimate can be significantly improved if the 3D structure of the CME plasma is known (e.g., from the 3D reconstruction with the polarisation-ratio method) [2, 3].

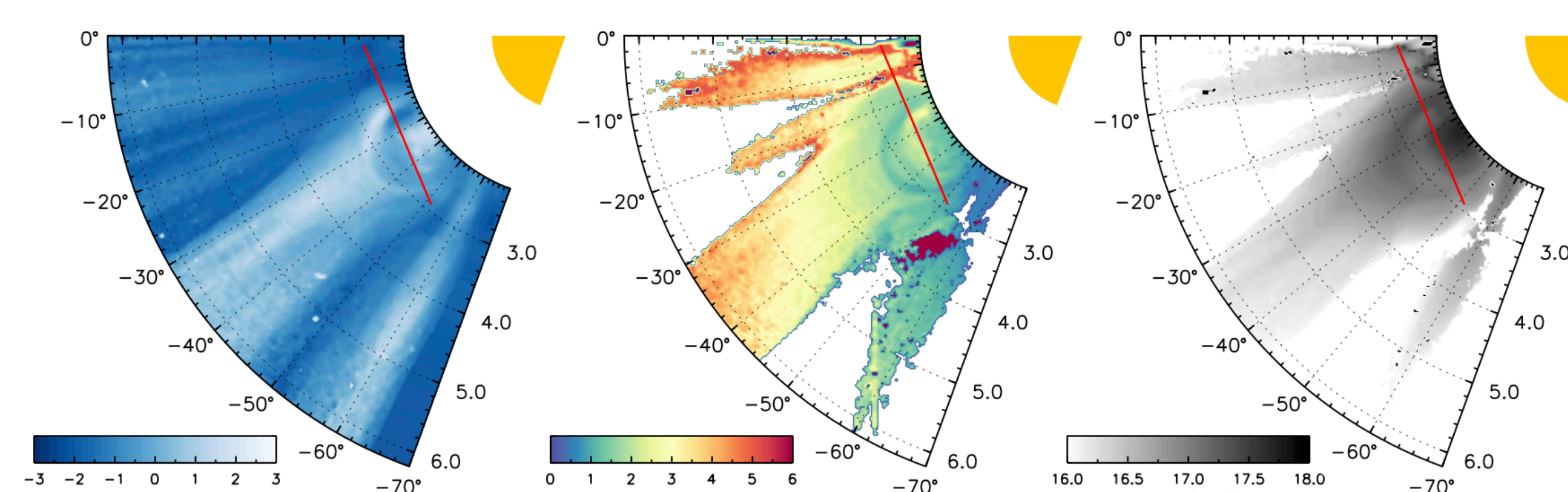


Figure 2. Topographical map of the electron column density within a CME observed by LASCO-C2 (right panel) obtained from the combination of the polarised brightness measurement (left panel) and the average location along the LOS of the CME plasma (middle panel) derived with the polarisation-ratio method.

## Erupting prominences

About 70% of CMEs are associated with erupting prominences. Modelling the radiative transfer processes out of local thermodynamic equilibrium (non-LTE) is fundamental to correctly retrieve the prominence plasma parameters.

We developed the diagnostics methods for erupting prominences using Lyman- $\alpha$  intensities from observed UVCS spectra, densities and flow velocities derived from visible-light images, and combining them in an iterative approach based on a 1D non-LTE radiative-transfer code (MALI; see Fig. 3) [5, 6, 7].

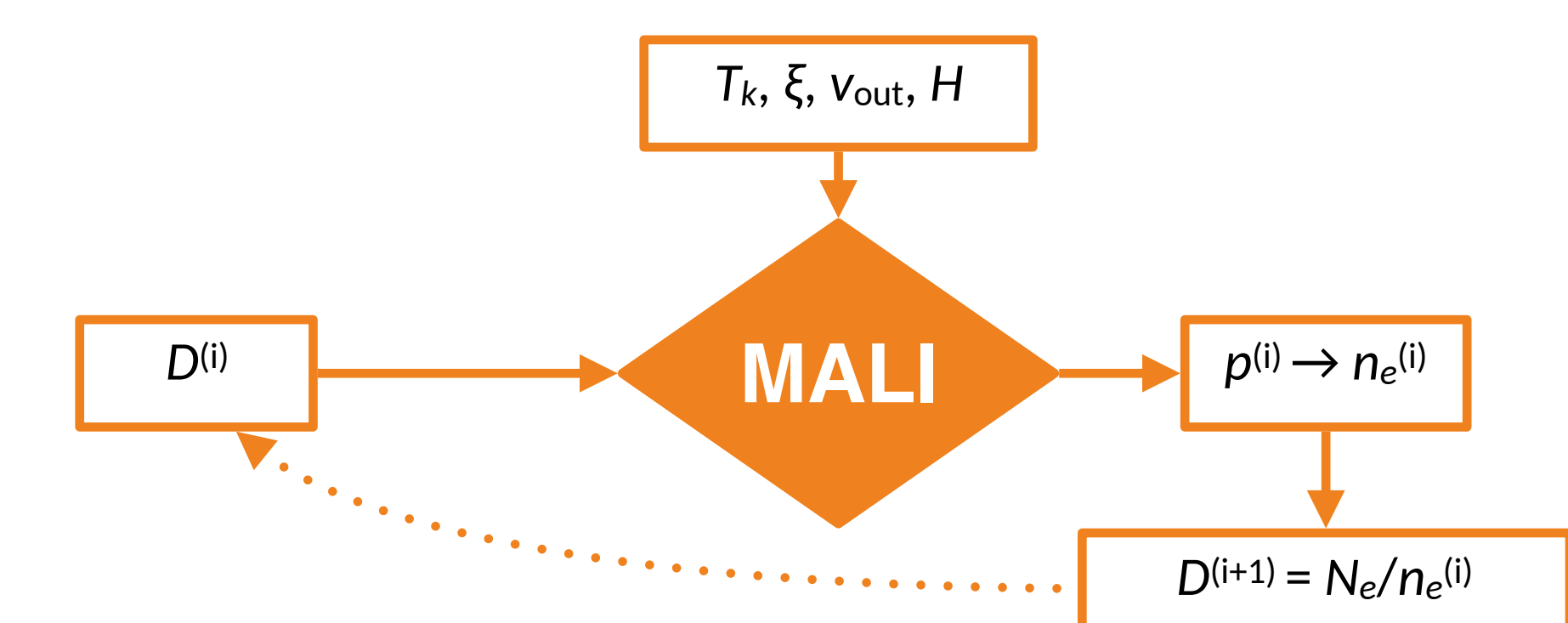
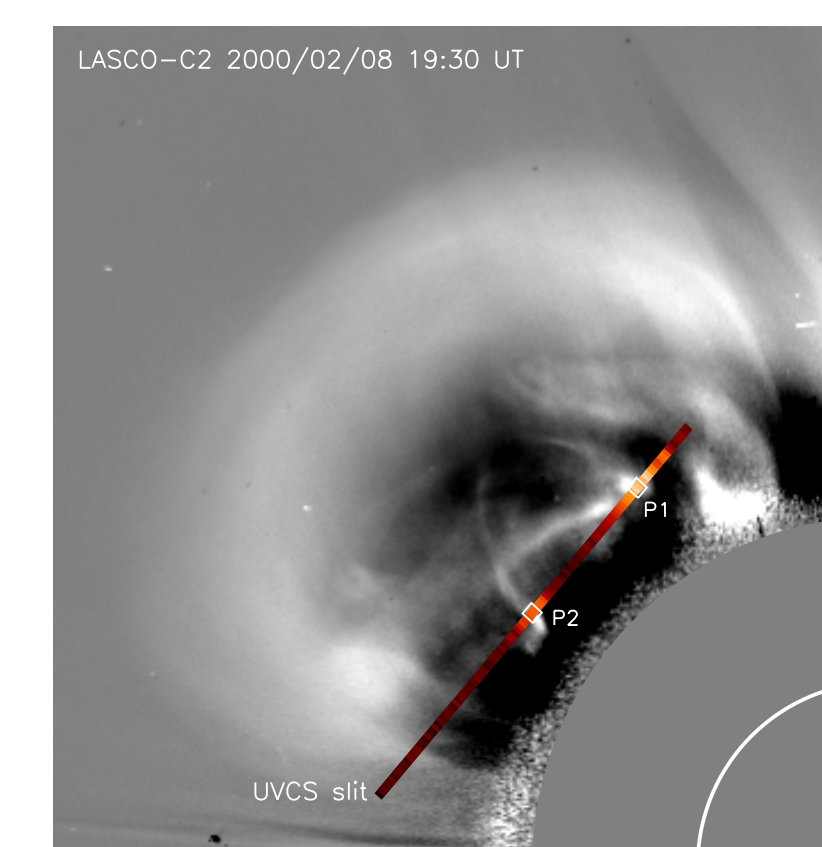


Figure 3. Left: erupting prominence observed simultaneously by LASCO-C2 in visible-light (base difference) and UVCS in Lyman- $\alpha$  (intensity along the slit). Right: scheme of the iterative diagnostic method based on the MALI code. Input parameters are: the prominence thickness  $D$ , kinetic temperature  $T_k$ , non-thermal velocities  $\xi$ , flow velocity  $v_{\text{out}}$ , height above the surface  $H$ . The output is the gas pressure necessary to reproduce the observed Lyman- $\alpha$  intensity.

Analysis of LASCO-C2 images and UVCS Lyman- $\alpha$  spectra of a “hot” prominence has shown that, despite the prominence is a low-pressure structure with low electron densities and high temperatures, up to 50% of the prominence is characterised by non-negligible optical thickness ( $> 0.3$ ) [5]. Combination of visible-light and UV data can be also be used to infer the prominence plasma filling factor [7].

## Diagnostics of coronal magnetic fields

Fast CMEs can drive shock waves expanding in the corona and heliosphere. Analysis of the dynamics of CME-driven shocks in visible-light images (see Fig. 4) can be used to infer the average magnetic field strength on the POS through the measurement of the shock geometry and velocity and the plasma compression ratio, which can be related to the Alfvén Mach number and the Alfvén velocity through simple MHD relationships [8].

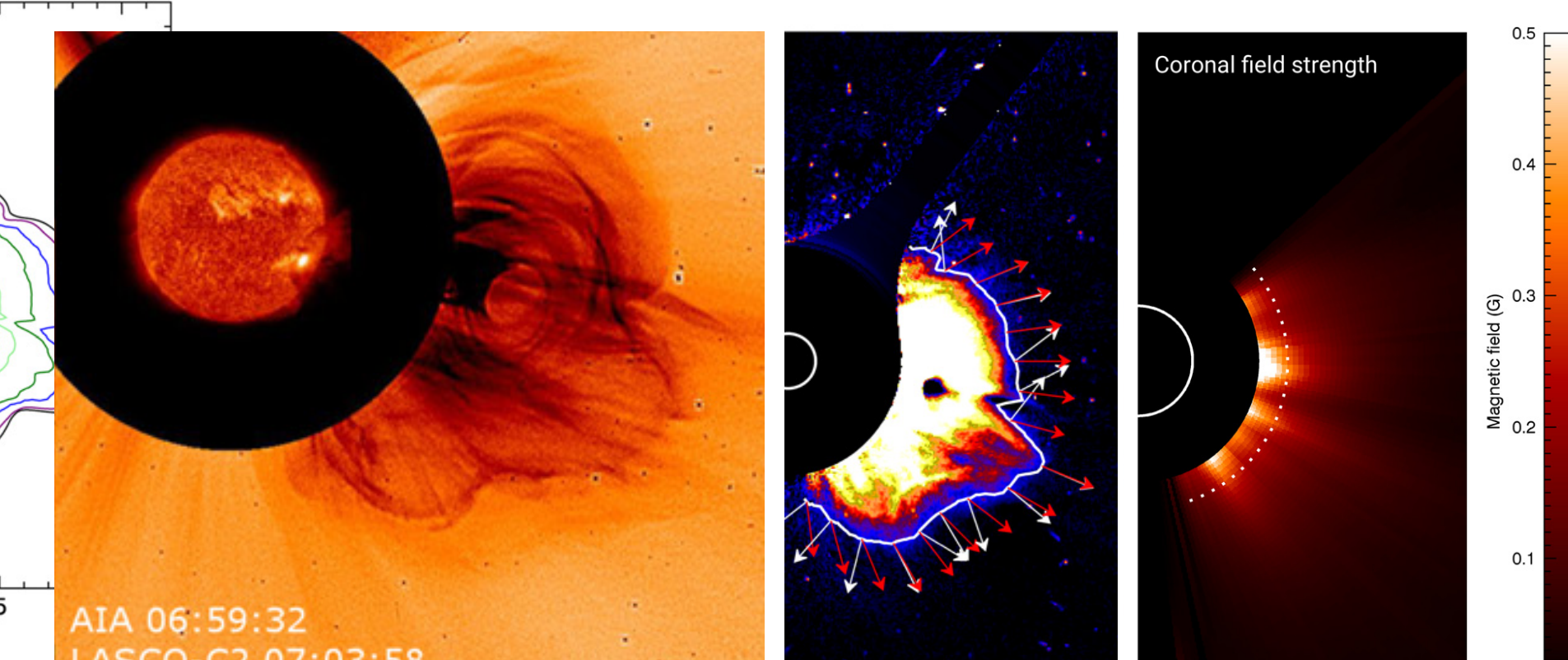


Figure 4. Map of the average coronal magnetic-field strength on the POS (right panel) derived from the analysis of the dynamics of a coronal shock driven by a CME observed and tracked in LASCO-C2 visible-light images (right and middle panels).

## Diagnostics of electron temperature

Combination of visible-light and Lyman- $\alpha$  observations can be used to estimate the CME plasma temperature taking into account the Doppler dimming effect that affects the resonantly scattered component of the Lyman- $\alpha$  emission line [2].

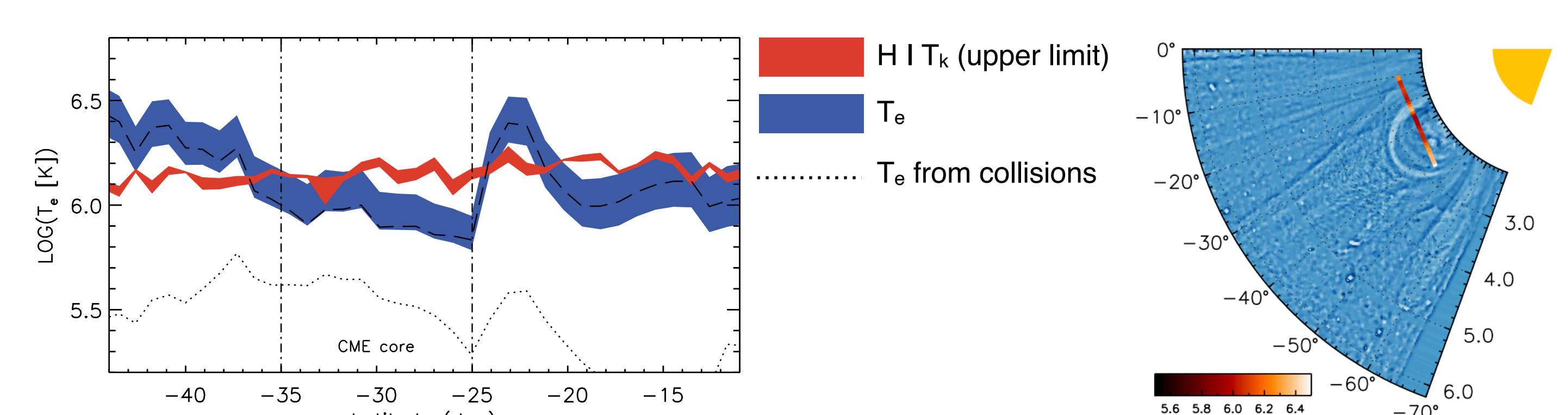


Figure 5. Left: Lyman- $\alpha$  temperature derived from UVCS spectra (red shaded area) compared with the electron temperature derived from the combined analysis of Lyman- $\alpha$  and visible-light observations (blue shaded area), plotted as functions of the heliographic latitude along the UVCS slit, for the same CME of Fig. 2. The vertical width of the areas is equal to the uncertainties affecting the results. Right: polar map of the polarised brightness (with radial filter) and the derived electron temperatures along the UVCS slit superimposed on the plot using color gradients.

From the analysis of three CMEs observed simultaneously by LASCO-C2 and UVCS, we found that temperatures derived from the combination of visible-light and UV data are consistent with previous estimates (see Fig. 5). CME cores are usually associated with cooler plasma, and a significant rise of temperatures is observed moving from the core to the front of the CME.

## References

- [1] Susino, R. et al. 2014, ApJ, 790, Issue 1, id. 25
- [2] Susino, R. & Bemporad, A. 2016, ApJ, 830, Issue 2, id. 58
- [3] Bemporad, A., & Pagano, P. 2015, A&A, 576, id. A93
- [4] Vourlidas, A. et al. 2000, ApJ, 534, 456
- [5] Heinzel, P. et al. 2016, A&A, 589, id. A128
- [6] Jejčič, S. et al. 2017, A&A, 607, id. A80
- [7] Susino, R. et al. 2018, A&A, 617, id. A21
- [8] Susino, R. et al. 2015, ApJ, 812, Issue 2, id. 119